

Nonlinear soil response as a natural passive isolation mechanism—the 1994 Northridge, California, earthquake

M. D. Trifunac & M. I. Todorovska

Civil Engineering Department, University of Southern California, Los Angeles, CA 90089-2531, USA

(Received 20 June 1997)

The spatial relationship between areas with severely damaged (red-tagged) buildings and areas with large strains in the soil (indicated by reported breaks in the water distribution system), observed during the 1994 Northridge earthquake, is analysed. It is shown that these areas can be separated almost everywhere. Minimal overlapping is observed only in the regions with very large amplitudes of shaking (peak ground velocity exceeding about 150 cm s^{-1}). One explanation for this remarkable separation is that the buildings on 'soft' soils, which experienced nonlinear strain levels, were damaged to a lesser degree, possibly because the soil absorbed a significant portion of the incident seismic wave energy. As a result, the total number of severely damaged (red-tagged) buildings in San Fernando Valley, Los Angeles and Santa Monica may have been reduced by a factor of two or more. This interpretation is consistent with the recorded peak accelerations of strong motion in the same area. It is concluded that significant reduction in the potential damage to wood frame single family dwellings may be expected in areas where the soil experiences 'large' strains (beyond the linear range) during strong earthquake shaking, but not significant differential motions, settlement or lateral spreading, near the surface. © 1997 Elsevier Science Ltd.

Key words: Northridge earthquake, damage, red-tagged buildings, water pipe breaks, ground strains, nonlinear soil response, passive isolation, structural control.

1 INTRODUCTION

The Northridge earthquake (17 January 1994, $M_L = 6.4$) occurred on a blind thrust fault below San Fernando Valley in the densely populated Los Angeles metropolitan area. The rupture was initiated at depth ($\sim 18 \text{ km}$) and then spread to north, north-west and up along the surface dipping 42° to south-west and striking at 122° . Many buildings, free-way structures and utilities were damaged.^{1–5} The characteristics of ground shaking at locations where damage was observed were estimated from smoothed contour maps of peak amplitudes of motion (acceleration, velocity and displacement), peak strain factor (v_{\max}/\bar{v}_s , where v_{\max} is the horizontal peak velocity of strong motion and \bar{v}_s is the average velocity of shear waves in the top 30 m of soil) and Pseudo Relative Velocity Spectrum amplitudes,^{6–9} drawn on the basis of more than 200 strong motion accelerograms recorded in the metropolitan area. This made it possible to relate the degree of damage to the amplitudes of

shaking. For example, the density (per km^2) of severely damaged (red-tagged) single family dwellings (SFD) could be correlated with peak velocity of strong motion.¹⁰ Further, buried water pipes are vulnerable to large strains and differential motion of the soil. In the developed areas, the density of breaks in the water pipes (per km^2) could be used as an indicator of the level of strain and/or of some form of soil failure.^{11,12} The density of water pipe breaks was correlated with estimates of the strain factor,¹² v_{\max}/\bar{v}_s . The derived functional relationships between the average density of red-tagged buildings and the peak ground velocity and between the average density of water pipe breaks and the peak strain factor can then be used to infer the range of peak ground velocity from the observed distribution of red-tagged buildings, and the range of the strain in the soil from the density of water pipe breaks. These relationships were used in this paper, to help interpret the observed spatial relationship between the areas with damaged (red-tagged) buildings and the areas with reported breaks in the water pipes.

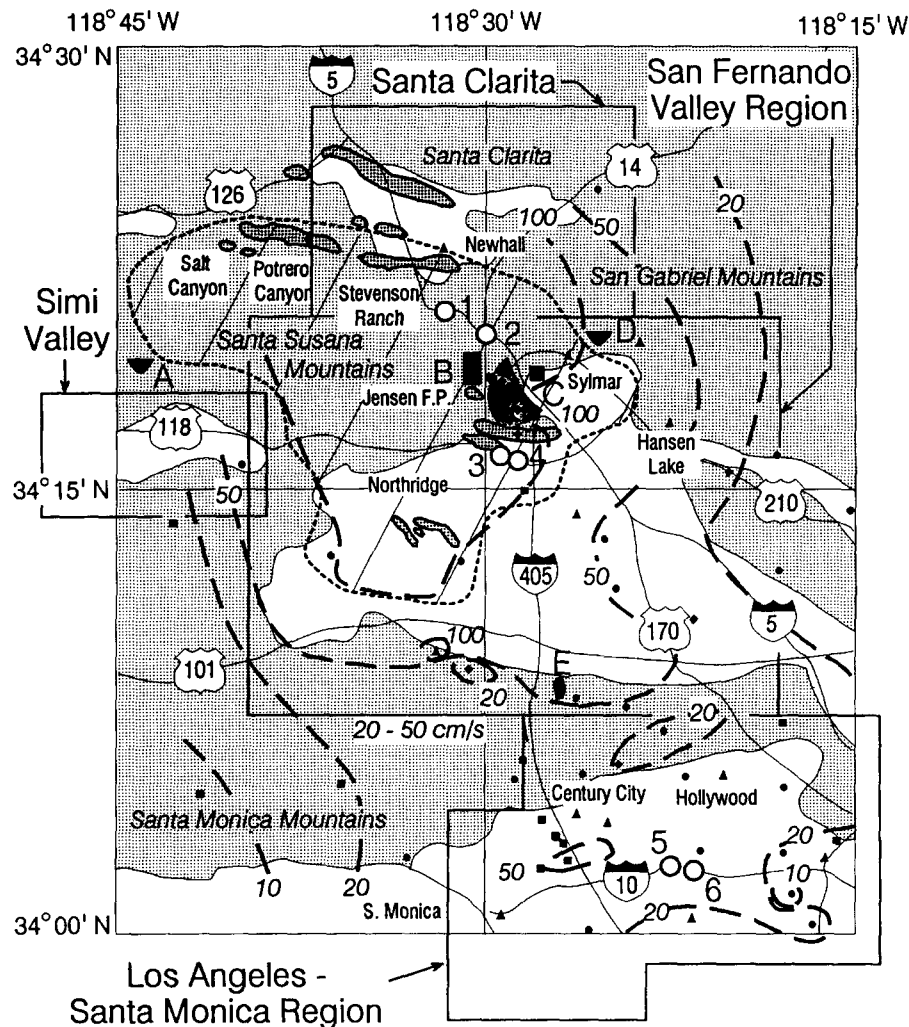


Fig. 1. The epicentral area of the Northridge earthquake (17 January 1994, $M_L = 6.4$). The short dashed line outlines the surface projection of the fault. The light gray areas indicate bedrock, and the white areas quaternary sediments. The triangular, circular, diamond and square symbols show the location of the strong-motion recording sites. The shaded regions outlined by heavy solid lines indicate zones of concentrated ground breakage: A—Simi Valley Tailings Dam; B—Jensen filtration plant; C—San Fernando Valley Juvenile Hall; D—Pacoima dam site; E—intersection of Mulholland Drv. and Beverly Glen Blvd. The open circles (sites 1 to 6) indicate locations of extensive damage or collapse of freeway structures. Heavy and long dashed lines show contours of horizontal peak velocity of strong ground motion, recorded in free-field. (Redrawn from Trifunac *et al.*, 1996.)

Fig. 1 summarizes the locations where major damage occurred in relation to the causative fault. The small triangular, diamond, circular and square symbols show the locations of the strong-motion sites. The shaded regions outlined by heavy solid lines indicate zones of concentrated ground breakage:³ A—Simi Valley Tailings Dam; B—Jensen filtration plant; C—San Fernando Valley Juvenile Hall; D—Pacoima dam site; E—intersection of Mulholland Drv. and Beverly Glen Blvd. The open circles indicate locations of extensive damage or collapse of freeway structures: 1—Gavin Canyon under-crossing; 2—Interstate 5 and SR14 interchange; 3—Mission Gothic under-crossing of SR118; 4—Bull Creek Canyon Channel bridge; 5—La Cienega—Venice under-crossing of Interstate 10; and 6—Fairfax—Washington under-crossing of Interstate 10. Smoothed contours of horizontal peak ground velocity⁷

are shown by heavy dashed and full lines. This figure also shows the San Fernando Valley, Los Angeles—Santa Monica, Santa Clarita and Simi Valley regions, referred to later in this text.

Before the deployment of dense strong-motion arrays (e.g. the Bear Valley array¹³ in 1972 and the Los Angeles and vicinity array⁶), the studies on spatial variation of strong-motion amplitudes were based on observation of damage to 'typical' residential buildings. The variety of construction methods and materials, actual strength and density of buildings per unit area, small areas covered by cities, and great variety of underlying geological and soil conditions worldwide, have contributed to intricate and often conflicting interpretations of the observed damage. The traditional belief that the earthquake damage is greater when the ground is poor overlooked the complexities of the

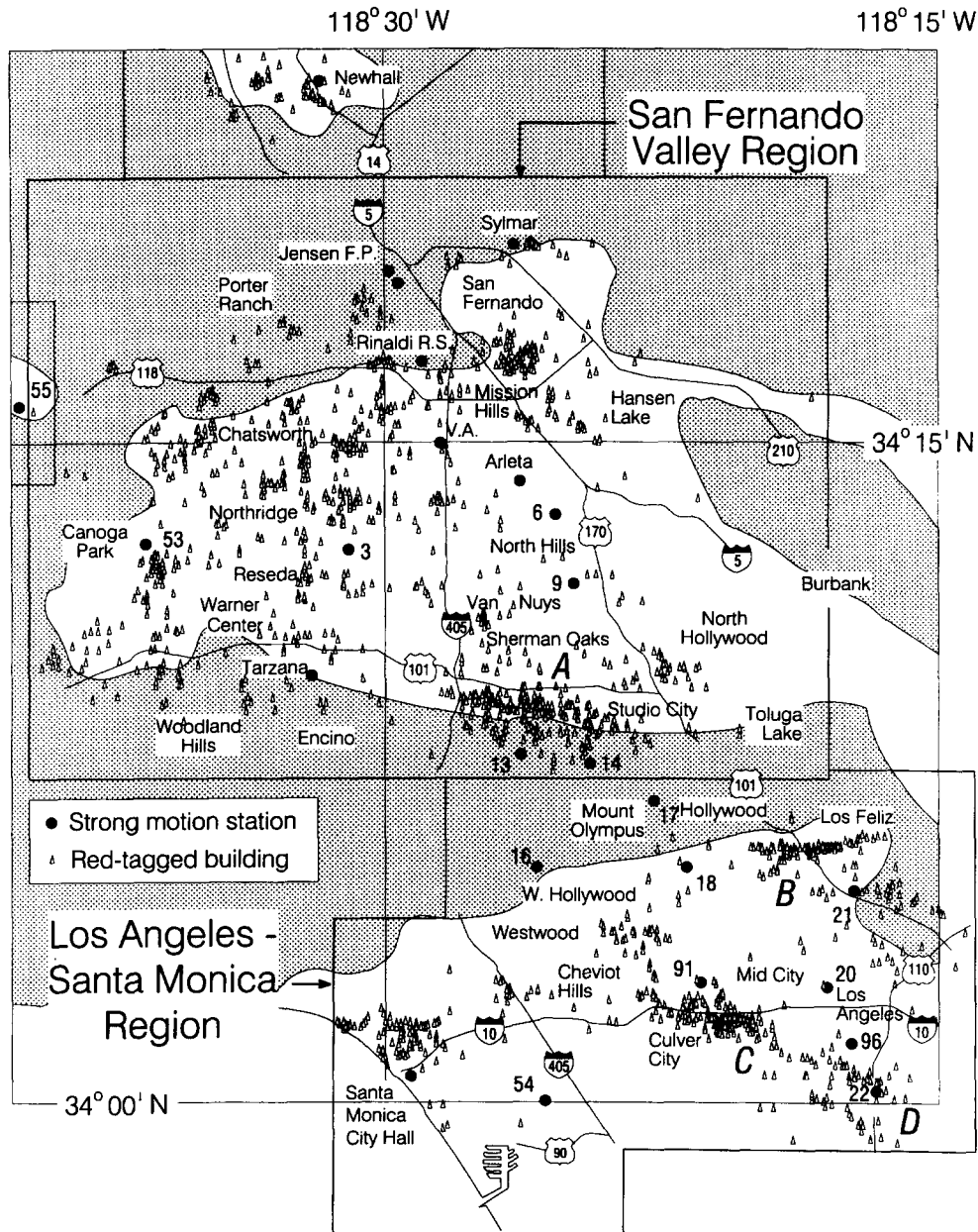


Fig. 2. Location of severely damaged (red-tagged) buildings (open triangles) during the Northridge earthquake in the San Fernando Valley and Los Angeles-Santa Monica regions. The solid circles show selected strong-motion recording stations.

transition from small (~linear) to large (beyond the linear range) response of soils and foundation materials, which further contributed to the complexities of this subject.

The first systematic studies of damage to Japanese wood houses (old style, with little or no diagonal bracing and on inadequate foundation) showed 'small' degree of damage for thickness of the surface soil layers up to several metres, and increasing degree of damage for deeper layers¹⁴ (5 to 50 m). The damage also increased with increasing Poisson's ratio in the soil, because the Japanese wood houses are sensitive to uneven settlement. The former is associated with damage caused by inertial forces, while the latter

results from large differential motions and thus belongs to a different (pseudo static) type of damage.

This paper shows that, for the Northridge earthquake, the areas with severely damaged buildings (red-tagged) and the areas where many breaks in pipes of the water distribution system were reported can be separated except in small regions where overlap occurs. The physical causes which lead to the observed distribution of damaged buildings are discussed, but quantitative analysis is out of the scope of this paper. Similar observations reported in the literature for other earthquakes are discussed, as are the implications of the observed phenomenon on seismic microzonation and building codes.

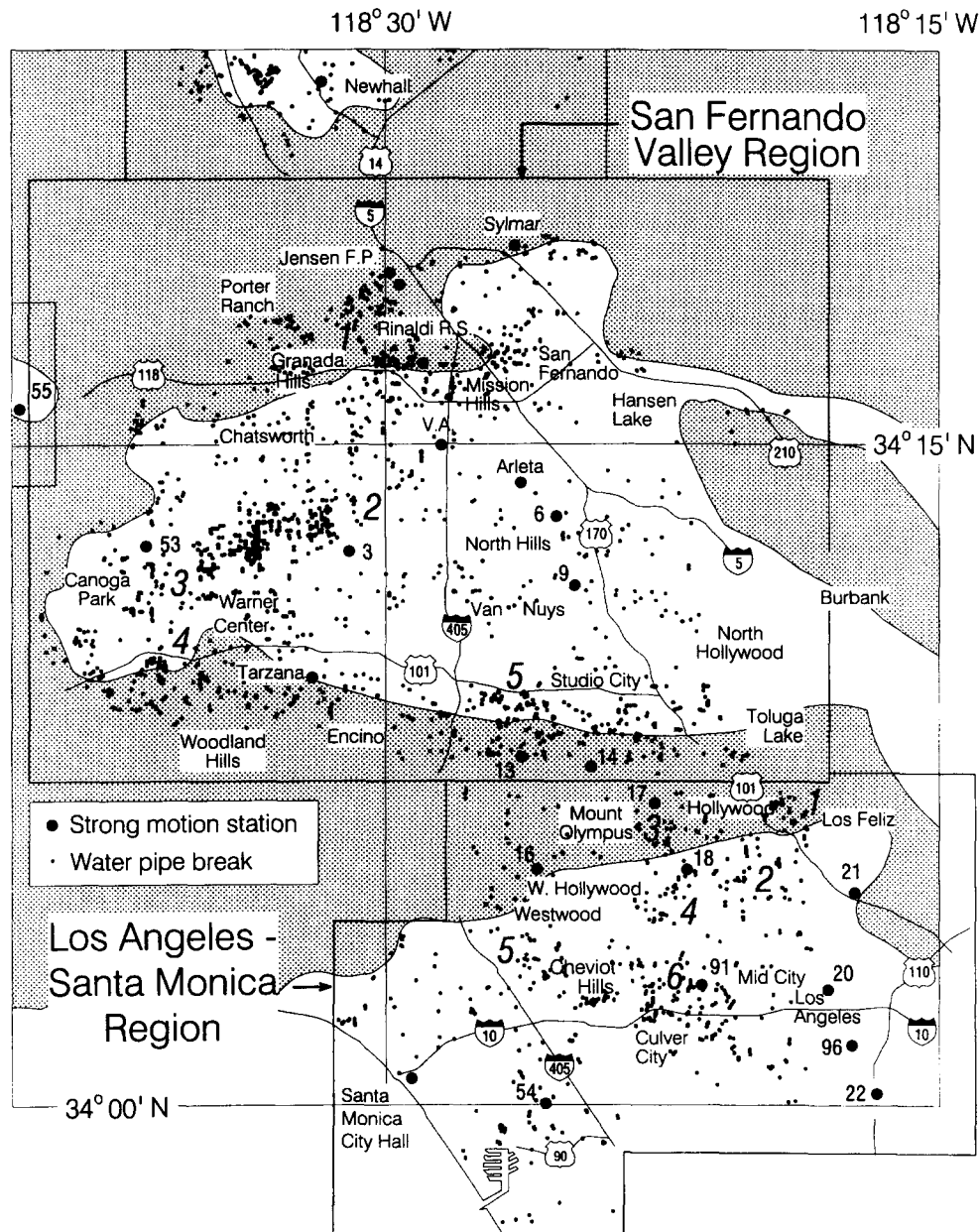


Fig. 3. Location of reported breaks in the pipes of the water distribution system (small solid dots) during the Northridge earthquake in the San Fernando Valley and Los Angeles-Santa Monica regions.

2 DAMAGE TO BUILDINGS AND GROUND STRAINS DURING THE NORTHRIDGE EARTHQUAKE

2.1 Damage data

Following the Northridge earthquake, the buildings were inspected by the Office of Emergency Services, administered by the Los Angeles Department of Building Safety.¹⁵ Those hazardous to life were 'red-tagged', the moderately damaged ones which posed no threat to life and whose occupants were allowed to enter to remove their possessions were 'yellow-tagged'. Those that did not pose any life safety

hazard to their occupants were green-tagged. One and a half months after the earthquake, the Los Angeles Department of Building Safety tagged more than 47 000 buildings. Of those, 88% were single family detached (SFD) buildings, 2% were single family attached (SFA), and 10% were low-rise multifamily (LRM) buildings. Red tags were posted onto 2% of SFD buildings, 3% of SFA buildings and 6% of LRM buildings.¹ Yellow tags were posted onto 11% of SFD buildings, 15% of SFA buildings and 16% of LRM buildings. Remaining (87% of SFD, 82% of SFA and 78% of LRM) buildings received green tags.

Fig. 2 shows the locations of red-tagged buildings in the San Fernando Valley and the Los Angeles-Santa Monica

regions. High concentration of damaged (red-tagged) buildings were observed: (A) along Ventura Blvd, between Laurel Canyon and San Diego (405) Freeway, in San Fernando Valley; (B) along Sunset Blvd, between Vermont and Highland Ave., in Hollywood; (C) along the Santa Monica (I-10) Freeway, between Crenshaw and Fairfax Blvd; and (D) near the intersection of Harbor (110) Freeway and Vernon, both in Los Angeles. The location of these regions is indicated by letters A to D in Fig. 2. Large numbers of red-tagged buildings were observed also in other areas of San Fernando, Canoga Park and Santa Monica. In this study, 949 red-tagged buildings in San Fernando Valley and 410 in Los Angeles are considered. In these two regions, the urbanized areas, with relatively uniform density of buildings (km^2), cover respectively 479 km^2 and 241 km^2 .

Soil failure, leading to breaks in water pipes, can be caused by faulting,¹⁶ landslides,^{17,18} liquefaction leading to ground fissures,¹⁹ lateral spreading and subsidence,²⁰ and by large strains and stresses associated with traveling ground waves.²¹ Many broken or leaking pipes were identified in the water distribution system in the areas affected by the shaking during the Northridge earthquake. The location of water pipe breaks is shown by dots in Fig. 3. Many of these breaks occurred in old brittle pipes, which could be damaged by ground motion and ground stains during the passage of seismic waves. The low frequency of such breaks per km^2 and their dispersed pattern suggest that many of these breaks were not caused by ground failure. The zones with concentrated groups and with large number of pipe breaks could be considered to have experienced some form of ground failure. In the San Fernando Valley region, such zones were in: (1) Granada Hills, (2) Northridge, (3) Canoga Park, (4) Woodland Hills, and (5) Sherman Oaks and Studio City. In the Los Angeles–Santa Monica region, such zones were in: (1) Hollywood, north of 101 Freeway, between Vine and Western; (2) Hollywood, along Highland; (3) Hollywood Hills, north of Sunset Blvd; (4) Hollywood, along La Cienega Boulevard; (5) Cheviot Hills, along Motor Ave.; and (6) along Santa Monica Freeway (Interstate 10), between La Cienega and La Brea. These zones are indicated in Fig. 3 by a number. In this paper, 1422 pipe breaks in San Fernando Valley and 362 breaks in the Los Angeles–Santa Monica regions are considered.

2.2 Analysis of the damage patterns

Concentration of damaged buildings in an area is a consequence of the complex interaction of many factors. First, it depends on the strong-motion amplitudes, which may be larger than expected (at that distance) because of focusing and reflection of seismic waves off the geologic basement and by topographic features, lateral reflection off the edges of sedimentary basins, amplification of waves propagating across sharp impedance changes, and focusing by the three-dimensional geometry of local soil deposits.⁹ It also depends on the duration of shaking, which controls the power of the

incoming wave energy. All these are influenced also by the three-dimensional geologic structure along the path of the waves between the earthquake source and the building site. Next, the concentration of damaged buildings depends on the density of structures, their type and ability to withstand strong shaking. More red-tagged buildings will be found in areas with greater number of old and deteriorated structures, and where heavy and brittle materials were used in the construction (e.g. unreinforced masonry structures).

In the following, it is assumed that it is possible to outline areas with no, with intermediate (yellow-tagged buildings), and with high (red-tagged buildings) levels of damage, by visual filtering and smoothing of the data points. To emphasize the areas with high concentrations of damaged buildings and to provide more contrast with respect to the areas with no damaged buildings, only the population of red-tagged buildings is considered, and is presented relative to the populations of the water pipe breaks. Drawing boundaries between the locations of damaged buildings and of pipe breaks will emphasize that this separation is indeed possible. These boundaries are not fixed, and will depend on the level and patterns of strong-motion amplitudes during a particular earthquake, and on the expansion and changes in settled areas, for example.

To simplify the presentation and to avoid clutter caused by many overlapping points, the sites of water pipe breaks will be shown by solid dots and the areas covered by red-tagged buildings by gray zones. Figs 4 and 5 show such plots for the San Fernando Valley and the Los Angeles–Santa Monica regions. It is seen that, with few exceptions (7% of all breaks in water pipes in Los Angeles and Santa Monica and 10% in San Fernando Valley), the gray areas do not overlap with the location of breaks in the water pipes.

By using empirical equations relating the density of red-tagged buildings with peak ground velocity,¹⁰ and density of pipe breaks with the strain factor¹² v_{\max}/\bar{v}_s , it is estimated that, within the areas enclosed by the solid lines in Figs 4 and 5, the peak ground velocity, v_{\max} , approached or exceeded 150 cm s^{-1} . It is seen in these figures that the areas where the location of pipe breaks overlaps with the gray areas coincides with these areas of high peak velocity.

Smooth interpolation of the contours of peak velocities during the Northridge earthquake (derived from recorded strong-motion accelerations) shows that the horizontal peak velocity exceeded 100 cm s^{-1} in Northridge, Reseda, Granada Hills, Mission Hills and in most areas of northeastern San Fernando Valley. In the other areas of the San Fernando Valley, the horizontal peak velocity was between 50 and 100 cm s^{-1} (Fig. 1). In Los Angeles, Hollywood and Century City, the smooth contours of peak horizontal velocity show a range of values, from 20 to 50 cm s^{-1} (Fig. 1). Through most of the San Fernando valley, the peak strain factor (v_{\max}/\bar{v}_s) was larger than $10^{-2.75}$, reaching $10^{-2.25}$ in Reseda and Mission Hills. In the Los Angeles–Santa Monica region, it was¹² between $10^{-3.25}$ and $10^{-2.75}$.

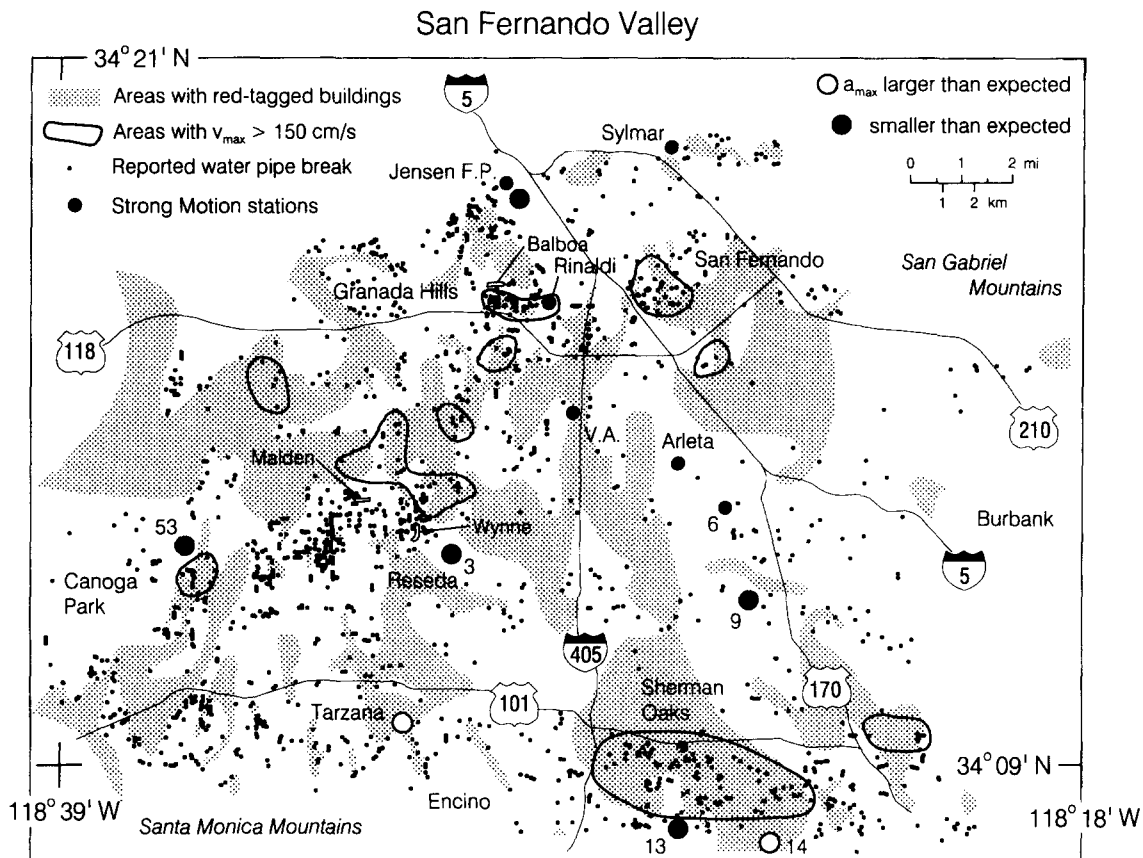


Fig. 4. San Fernando valley region. Spatial relationship of the areas with severely damaged buildings (gray zones) and the areas with large surface strain (indicated by locations of reported breaks in water pipes). The closed continuous contours outline zones where the peak ground velocity may have been close to or above 150 cm s^{-1} .

2.3 Interpretation of the observed damage patterns

The results in Figs 4 and 5 can be interpreted as follows. In most (more than 90%) of the gray areas (location of red-tagged buildings), where the peak ground velocity did not exceed 100 to 150 cm s^{-1} , the soil response during the strong shaking was 'essentially linear', and most of the incident seismic wave energy could be transmitted into and severely damage many buildings (red-tagged buildings). In the area outside the gray zones, the soil responded in a nonlinear fashion, to a degree which is reflected in the density of breaks in the water pipes. In this process, the soils appear to have absorbed part of the incident wave energy, which would otherwise be available for excitation and destruction of the buildings. Certainly, some damage to structures did occur in those areas (yellow-tagged buildings), but no buildings were red-tagged.

Detailed analyses of different mechanisms resulting in large soil stains, differential motion and soil failure are beyond the scope of this paper. In some areas, the failure mode can be suggested on the basis of simple field observations,⁵ can be inferred from detailed *in situ* testing (Malden St., Wynne Ave. and Balboa Blvd;²² see Fig. 4), or are suggested by simple theoretical models (e.g. 'fluidization'²¹). Trifunac and Todorovska¹² overlaid the areas with 'high

soil strain' (high density of water pipe breaks) with areas of known distribution of Holocene deposits and with areas of high liquefaction susceptibility, but found no obvious trends or correlation. Apparently, new and innovative field observations and measurements need to be carried out in future to be able to predict locations of 'weak soil zones' which would absorb seismic wave energy during future earthquakes and reduce severe damage of typical residential buildings.

In San Fernando Valley and in the Los Angeles–Santa Monica regions, respectively $\sim 10\%$ and $\sim 7\%$ of all pipe breaks occurred within the gray zones. With few exceptions, these areas coincide with the zones which are believed to have experienced peak ground velocity $v_{max} \geq 150 \text{ cm s}^{-1}$.¹⁰ Assuming a typical value for the average shear wave velocity in the top 30 m of soil $\bar{v}_s \approx 300 \text{ m s}^{-1}$ and $v_{max} = 150 \text{ cm s}^{-1}$, would imply strain factors greater than $10^{-2.3}$ at 'soft' soil sites. At stations USC 53, USC 03, Jensen Filtration Plant (Administration Building), USC 09 and USC 13 (shown by larger symbols in Fig. 4), the strain factors were larger than $\sim 10^{-2.8}$, and the recorded peak accelerations were reduced by 0.3 to 0.4g relative to the average trends at stiff soil sites and at comparable distances from the causative fault, implying nonlinear site response.¹¹ For these large strains, and beyond, distortion and warping of the foundation is expected to

Los Angeles - Santa Monica

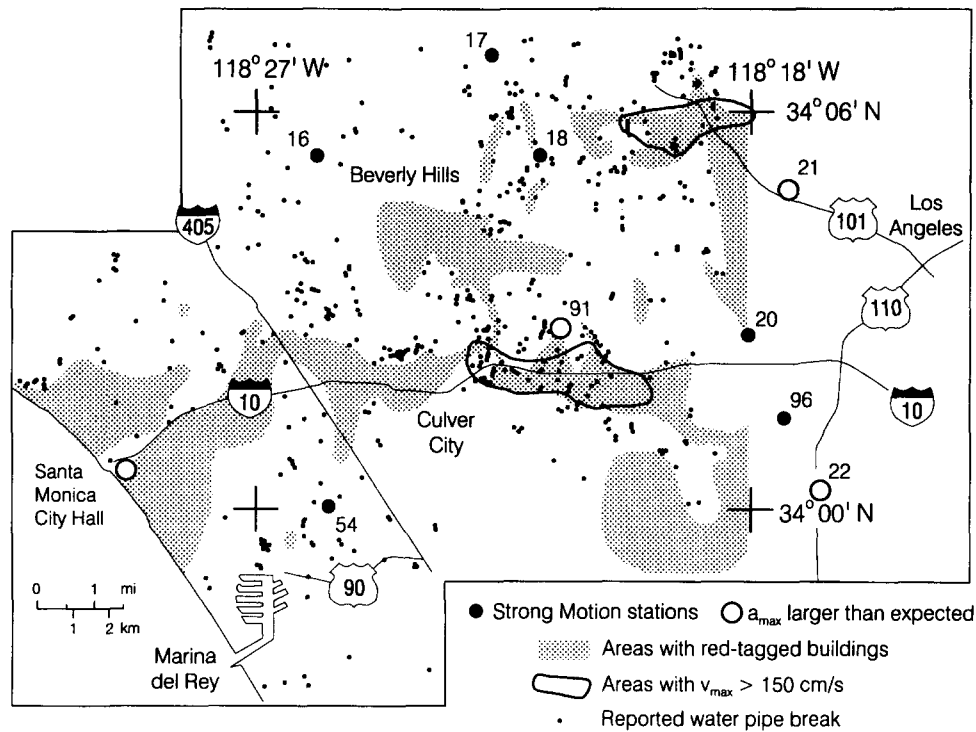


Fig. 5. Los Angeles–Santa Monica Region. Spatial relationship of the areas with severely damaged buildings (gray zones) and the areas with large surface strain (indicated by locations of reported breaks in water pipes). The closed continuous contours outline zones where the peak ground velocity may have been close to or above 150 cm s^{-1} .

contribute to the damage of structures via pseudo static deformation.

For completeness of this presentation, the distribution of red-tagged buildings (gray zones) and breaks in the water

pipes in Santa Clarita and in Simi Valley are also presented (Figs 6 and 7). The results are consistent with the preferred interpretation, but the extent and ‘less uniform density’ of developed areas in these regions are not sufficient to

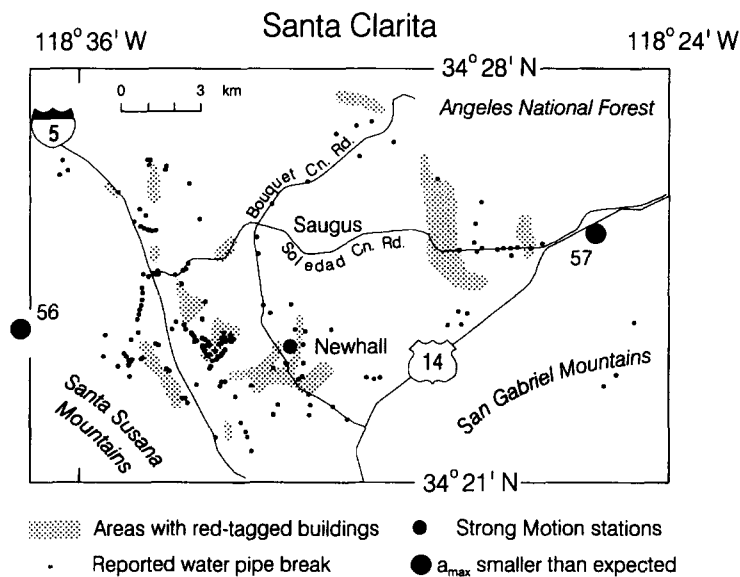


Fig. 6. Santa Clarita region. Spatial relationship of the areas with severely damaged buildings (gray zones) and the areas with large surface strain (indicated by locations of reported breaks in water pipes).

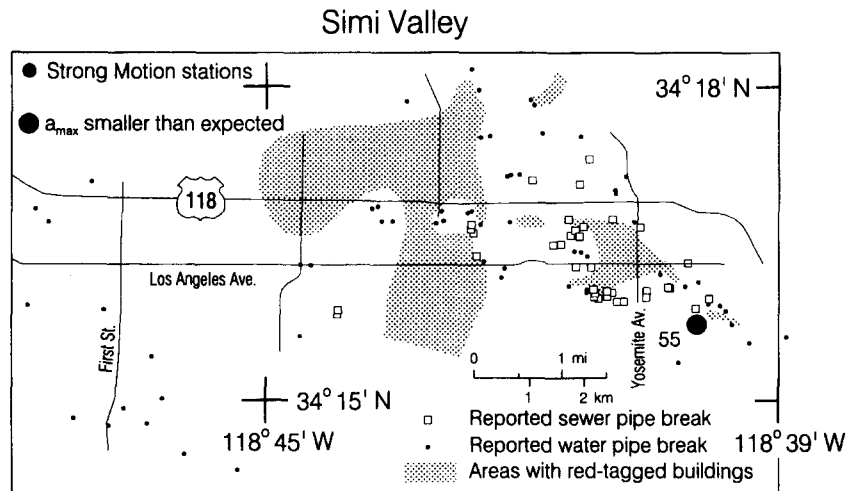


Fig. 7. Simi Valley region. Spatial relationship of the areas with severely damaged buildings (gray zones) and the areas with large surface strain (indicated by locations of reported breaks in water pipes).

confirm independently the above observations and interpretations made for the San Fernando Valley and the Los Angeles–Santa Monica regions (Figs 4 and 5).

3 DISCUSSION AND CONCLUSIONS

3.1 Benefits and drawbacks from nonlinear soil response

The degree to which the areas with apparent nonlinear soil response (indicated by the occurrence of breaks in the water pipe system), and the areas with high concentration of damaged buildings (red-tagged buildings) can be separated (for the Northridge earthquake damage data) is remarkable. This suggests that, via nonlinear response, soft soils may absorb a sufficient amount of seismic wave energy to reduce the damage to typical wood frame (SFD) buildings. Judging from the end result, during the Northridge earthquake, the nonlinear soil response may have been responsible for at least a twofold reduction of the number of red-tagged buildings in the areas studied (San Fernando Valley and Los Angeles–Santa Monica).

In general, the above phenomenon is complex and its usefulness is limited, because structures with ‘strong’ foundations may settle or tilt, while those on ‘weak’ foundations may be damaged by warping and twisting of the foundation during passage of strong-motion waves.²³ Still, there exists a window of opportunity where the beneficiary effects of nonlinear soil response are significant, while the adverse effects are still small. A preferred interpretation in this paper is that, for the Northridge earthquake, this window occurred for wood frame structures where the peak ground velocities were in the range from about 20 to 30 cm s^{-1} to about 100 to 150 cm s^{-1} . For peak velocities beyond that range, the strains and the differential motions in the soil will be large, and pseudo static deformation of the

foundation, partial settlement, and lateral spreading will contribute to or may dominate in causing the overall damage. Fortunately, the size of areas with very large peak velocities ($v_{max} > 150 \text{ cm s}^{-1}$) is expected to be small and thus, in a statistical sense, the damage from pseudo static deformation of building foundations should not pose a major problem.

3.2 Likelihood of the benefits and drawbacks during future earthquakes

The largest peak ground velocity recorded during the Northridge earthquake was $v_{max} \sim 160 \text{ cm s}^{-1}$, at the Rinaldi Receiving Station.²⁴ Prior to this earthquake, the largest recorded peak velocity was $v_{max} \sim 110 \text{ cm s}^{-1}$, at the Pacoima Dam site during the San Fernando, California, earthquake of 1971 ($M = 6.4$). On the basis of what is known about stress drop during shallow large earthquakes, it is not likely that v_{max} will often exceed 150 to 200 cm s^{-1} in large areas surrounding the source.^{25,26}

The observations reported in this paper are specific to the type of construction typical for single family detached (SFD) buildings in San Fernando and the Los Angeles–Santa Monica regions,⁴ and for the distribution of soil types in the same area. It could be expected that the same beneficial effects of soft soils (acting as a natural mechanism for passive isolation of SFD) would apply elsewhere. However, the range of peak velocities for which this would occur and the damage reduction factors are expected to change with the local conditions. Because of the lack of knowledge and data on the mechanisms contributing to nonlinear soil response during strong earthquake shaking, mapping areas where such a reduction will occur during future earthquakes does not seem feasible in the near future. However, it may be assumed that in the Los Angeles metropolitan area, within about 20 to 30 km from the earthquake source, and for similar soil conditions, ‘soft’

soil will reduce the strong-motion energy reaching the ground surface.

A preliminary analysis shows that, excluding the slopes of Santa Monica, San Gabriel, Santa Susana and Verdugo mountains (represented by quaternary sedimentary and volcanic rocks), the overall density of damaged buildings, relative to the density of breaks in water pipes, is smaller only at sites on the late Holocene silts and clays (age less than 1000 years, thickness 0 to 3 m). However, the lack of more obvious and simple spatial correlation between the areas which experienced some form of nonlinear site response, and of mapped distribution of Holocene deposits, or of the areas interpreted to have high liquefaction susceptibility,¹² for example, should be of some concern, for engineering analyses dealing with site-specific response. Apparently, in San Fernando Valley and in Los Angeles, typical 'soft' soil sites on recent Holocene deposits can respond to earthquake shaking in essentially linear manner. Since the probability of this occurrence is not small, we are faced with the challenge of discovering practical and reliable engineering methods for predicting the outcome during future earthquakes.

The relative abundance of strong-motion recordings of the Northridge earthquake made it feasible to define non-parametric attenuation functions for peak acceleration versus distance specific for this earthquake.¹¹ These functions show that peak accelerations at 'soft sites' (average shear wave velocity in the top 30 m of soil $\bar{v}_s < 360 \text{ m s}^{-1}$) begin to saturate around 0.4g, while continuing to grow at the sites with more 'rigid' surface materials ($\bar{v}_s > 360 \text{ m s}^{-1}$). The sites where the horizontal peak accelerations were larger than the average trend (Tarzana, USC 14, Santa Monica City Hall, USC 91, USC 21, USC 22) fall near or within the gray zones in Figs 4 and 5. The variations of the spatial distribution of strong-motion amplitudes which result from radiation pattern, fault mechanism, directivity, focusing, reflection and interference^{8,9} are apparently further complicated by complex irregular patterns of linear and nonlinear site response. The consequences of this last effect on our understanding and interpretation of the coherence of strong-motion amplitudes, differential motions at high frequencies, and the description and classification of local site effects²⁷ are far reaching and cannot be ignored. To understand the possible consequences, and to exploit them for the benefit of safer, more economical and more rational design of earthquake-resistant structures, new and innovative ways of data recording, analysis and interpretation must be developed, well beyond the current state-of-the-art in strong-motion geotechnical engineering.

3.3 Observations during other earthquakes

The long intervals between destructive earthquakes, the variations in the position of their foci, and the rapid growth of metropolitan areas make it difficult to repeat and to test previous findings. As with many other complex phenomena, when a new interpretation can be guided by observations

alone, a large number of data points is necessary to reveal the governing physical mechanisms. Thus, it is not surprising to find reports with conflicting or incomplete interpretations, as well as convergence towards simplistic, 'main stream' interpretation.

In old Tokyo city, during the great Kanto earthquake of 1923, the ratio of totally destroyed to partially destroyed wooden houses was about 1 for sites on alluvium and 4.5 for sites on diluvium and tertiary.¹⁴ The damage to brick buildings was approximately two times larger on 'soft ground' relative to 'very soft ground' and about three times greater on 'hard' ground than on 'very soft ground'. The damage and total destruction rates for reinforced concrete buildings showed decreasing trends with increasing thickness of the alluvial layer, between 0 and 30 m. During the 1933 Long Beach earthquake, masonry buildings with two and three stories experienced about two times greater damage on 'hard ground' than on 'soft ground,' while the damage to one-story buildings was about the same.¹⁴ Those and many other similar observations, made long before the strong-motion records became available, essentially assumed that the incident waves had about the same amplitudes and that the amplification or deamplification of incident motion would occur only locally. Thus the observed trends²⁸ could be challenged, but not ruled out, by assuming different nonuniform amplitudes of strong motion.²⁹

During 'nondestructive' earthquakes, water pipes can be damaged, but no structural damage is reported (e.g. the 1917 and the 1918 earthquakes felt in Kofu, Yamanashi Prefecture, Japan¹⁴). In Tokyo, during the Kanto earthquake of 1923, the pipes in the depth range from 1.8 to 2.4 m were most damaged, while the pipes shallower than 1.5 m or deeper than 3 m had almost no damage. The distribution and density of water pipe breaks in the epicentral region of the Northridge earthquake (Fig. 3) shows that some yielding took place in the shallow soil, and that linear methods of analysis are not valid there.

3.4 Implications for microzoning and seismic design codes

Nontectonic ground fractures, slumping, fissures and displacements on bedding planes and joints of sedimentary layers are common in epicentral regions of shallow earthquakes, and imply nonlinear deformation and failure, which limit the amplitudes of accelerations and velocities at the ground surface. Consolidated clay of low plasticity may be incapable of transmitting acceleration greater than about 0.2g, while medium dense sands might transmit 0.6g. Gravels and dry dense sands may transmit larger peak accelerations. Thus, for smaller amplitude excitation, soil deposits will behave 'elastically' and may amplify the incident wave motion. As the strength of the material decreases or as the incident motions increase, the soil will begin to yield and the peak accelerations will not be large near the ground surface.¹¹ Therefore, the linear methods used in

regionalization studies (microtremors, small earthquakes, distant earthquakes, aftershocks, amplitudes of coda waves) are not valid in epicentral regions where the site does not behave elastically. To be useful for engineering applications, seismic microzones must be shown (1) to dominate in determining the local variations in the wave amplitudes, (2) to be associated with the local geologic and soil properties and (3) to be consistent with recurring earthquake shaking.

In the light of the above discussion, one may wonder why so many earthquake design codes recommend larger base shear coefficients for soils of decreasing strength. Should damage caused by lateral spreading, settlement and tilting be analysed via larger inertial forces? For large strains, but 'linear' motion, the effects of differential motions and of inertial forces in long and stiff structures can be combined via SDC spectra,³⁰ but this approach must be modified and generalized when the foundation soil is expected to experience nonlinear response and permanent relative displacements.

3.5 Summary and conclusions

The patterns of spatial distribution of red-tagged buildings and of breaks in water pipes caused by the 1994 Northridge earthquake in typical residential neighborhoods were studied. Red-tagging is an indicator of severe damage of the predominantly wood frame single family detached dwellings, and the concentration of breaks in the water pipes is an indicator of nonlinear soil response or soil failure. Two regions were studied, San Fernando Valley and Los Angeles–Santa Monica region (Figs 1–3). Data from two more regions are presented (Santa Clarita and Simi Valley), but they are not sufficient to support independently the conclusions drawn from the analysis of the other two regions. The analysis showed that the areas with high concentration of red-tagged buildings do not overlap with the areas with breaks in water pipes, except where the peak ground velocity is estimated to have exceeded 100 to 150 cm s⁻¹. One interpretation of this is that the soft soils, responding nonlinearly and absorbing a portion of the incident seismic wave energy, acted as a passive isolation mechanism and led to a reduction in severe damage to the typical buildings in the areas studied. In the areas where the zones with red-tagged buildings and breaks in water pipes overlap (peak ground velocity exceeding 100 to 150 cm s⁻¹), the beneficial effect of the soft soils was overpowered by severe damage caused by large differential motions, settlement and failure of the foundation material.

It is concluded that, close to the earthquake source, soft soils responding nonlinearly to strong ground shaking may have a beneficial effect on structures. This will depend on the region, type of soil, type of buildings and amplitudes of shaking. The complex patterns of the observed damage, resulting from linear versus nonlinear soil response, should be considered in microzonation studies, but cannot be predicted by using weak motions (e.g. microtremors, coda

waves and weak motions from aftershocks). New research needs to be initiated focused on understanding the mechanism of the observed reduction of damage due to nonlinear soil response, the conditions under which it occurs, predictability during future earthquakes and how to avoid the adverse effects. The next step would be implementation of the results in zoning and seismic design codes as well as in earthquake loss estimation methodologies.

REFERENCES

1. U.S. Department of Housing and Urban Development, Assessment of damage of residential buildings caused by the Northridge earthquake. Report HUD-1499-PDR, USDHUD, 451 7th Street S.W., Washington DC, 1994.
2. City of Los Angeles Department of Water and Power, Repair reports showing locations of water pipe breaks and leaks in the distribution system, 1994.
3. Earthquake Engineering Research Institute, Northridge earthquake of January 17, 1994. Preliminary Reconnaissance Report, EERI 94-01, Oakland, CA, 1994.
4. Earthquake Engineering Research Institute, Wood buildings. Ch. 6 in Suppl. C to Vol. 11 of *Earthquake Spectra*, Northridge Earthquake Reconnaissance Report, Vol. 2, 1996.
5. Stewart, J. P., Bray, J. D., Seed, R. B. & Sitar, N., Preliminary report on the principal geotechnical aspects of the January 17, 1994, Northridge earthquake. Report No. UCB/EERC-94/08, Earthquake Engineering Research Center, Univ. of California, Berkeley, CA, 1994.
6. Trifunac, M. D., Todorovska, M. I. and Ivanović, S. S. A note on distribution of uncorrected peak ground accelerations during the Northridge, California, earthquake of 17 January, 1994. *Soil Dynamics and Earthquake Engineering*, 1994, **13**(3), 187–196.
7. Trifunac, M. D., Todorovska, M. I. and Ivanović, S. S. Peak velocities and peak surface strains during the Northridge, California, earthquake of 17 January 1994. *Soil Dynamics and Earthquake Engineering*, 1996, **15**(5), 301–310.
8. Todorovska, M. I. and Trifunac, M. D. Amplitudes, polarity and time of peaks of strong ground motion during the 1994 Northridge, California, earthquake. *Soil Dynamics and Earthquake Engineering*, 1997, **16**(4), 235–258.
9. Todorovska, M. I. and Trifunac, M. D. Distribution of pseudo spectral velocity during the Northridge, California, earthquake of 17 January, 1994. *Soil Dynamics and Earthquake Engineering*, 1997, **16**(3), 173–192.
10. Trifunac, M. D. and Todorovska, M. I. Northridge, California, earthquake of 1994: density of red-tagged buildings versus peak horizontal velocity and site intensity of strong motion. *Soil Dynamics and Earthquake Engineering*, 1997, **16**(3), 209–222.
11. Trifunac, M. D. and Todorovska, M. I. Nonlinear soil response—1994 Northridge, California, earthquake. *J. of Geotechnical and Geoenvironmental Engineering*, ASCE, 1996, **122**(9), 725–735.
12. Trifunac, M. D. and Todorovska, M. I. Northridge, California, earthquake of 1994: density of pipe breaks and surface strains. *Soil Dynamics and Earthquake Engineering*, 1997, **16**(3), 193–207.
13. Dielman, R. J., Hanks, T. C. and Trifunac, M. D. An array of strong motion accelerographs in Bear Valley, California. *Bulletin of the Seismological Society of America*, 1975, **65**, 1–12.
14. Kanai, K., *Engineering Seismology*. Univ. of Tokyo Press, Tokyo, Japan, 1983.

15. Los Angeles Department of Building Safety, Earthquake damage sites, January 17, 1994, in the City of Los Angeles. Map Prepared by Land Development and Mapping Division, City of Los Angeles, CA, 1994.
16. McCaffrey, M. A. and O'Rourke, T. D. Buried pipeline response to reverse faulting during 1971 San Fernando earthquake.. *Earthquake Behavior and Safety of Oil and Gas Storage Facilities, Buried Pipelines, and Equipment*, 1983, **77**(PVP), 151–159.
17. Fallgren, R. B. & Smith, J. L., Ground displacement at San Fernando valley Juvenile Hall during San Fernando earthquake. In *San Fernando California Earthquake of February 9, 1971*, Vol. 3. U.S. Dept of Commerce, NOAA, Washington, DC, 1973, pp. 189–196.
18. Youd, T. L., Ground movements in Van Norman Lake vicinity during San Fernando, California Earthquake of February 9, 1971. In *San Fernando California Earthquake of February 9, 1971*, Vol. 3. U.S. Dept of Commerce, NOAA, Washington, DC, 1973, pp. 197–206.
19. McCulloch, D. S. & Bonilla, M. G., Effects of the earthquake of March 27, 1964, on the Alaska railroad. U.S. Geological Survey Professional Paper 545-D, 1970.
20. Schussler, H., *The Water Supply of San Francisco, California*, M.B. Brown Press, New York, NY; Government Printing Office, Washington, DC, 1906, 161 pp.
21. Richards, R., Elms, D. G. and Budhu, M. Dynamic fluidization of soils. *J. of Geotechnical and Geoenvironmental Engineering, ASCE*, 1990, **116**(5), 740–759.
22. Holzer, T. L., Bennett, M. J., Tinsley, J. C., Ponti, D. J. & Sharp, R. V., Causes of ground failure in alluvium during the Northridge, California, earthquake of January 17, 1994. In *Proc. 6th U.S.–Japan Workshop of Earthquake Resistant Design of Lifeline Facilities and Counter Measures for Soil Liquefaction*, Tokyo, Japan, 1996.
23. Richards, R. Discussion of paper 'Nonlinear soil response, 1994, Northridge, California, earthquake', by M. D. Trifunac and M. Todorovska. *J. of Geotechnical and Geoenvironmental Engineering, ASCE*, 1997, **123**(10), 988–989.
24. Trifunac, M. D., Todorovska, M. I. & Lee, V. W., The Rinaldi strong motion accelerogram of the Northridge, California, earthquake of 17 January, 1994. *Earthquake Spectra*, 1998 (in press).
25. Trifunac, M. D. Preliminary analysis of the peaks of strong earthquake ground motion—dependence of peaks on earthquake magnitude, epicentral distance and the recording site conditions. *Bulletin of the Seismological Society of America*, 1976, **66**, 189–219.
26. Trifunac, M. D., Broad band extension of Fourier amplitude spectra of strong motion acceleration. Report No. CE 93-01, Dept of Civil Engineering, Univ. of Southern California, Los Angeles, CA, 1993.
27. Trifunac, M. D. How to model amplification of strong earthquake motions by local soil and geologic site conditions. *Earthquake Engineering and Structural Dynamics*, 1990, **19**(6), 833–846.
28. Martel, R. R., A report on earthquake damage to type III buildings in Long Beach. In *Earthquake Investigations in California 1934–1935*. U.S. Dept of Commerce, Coast and Geodetic Survey, Special Publication No. 201, 1936, Ch. 8.
29. Campbell, K. W. A note on the distribution of earthquake damage in Long Beach, 1933. *Bulletin of the Seismological Society of America*, 1976, **66**, 1001–1006.
30. Trifunac, M. D. and Todorovska, M. I. Response spectra for differential motion of columns. *Earthquake Engineering and Structural Dynamics*, 1997, **26**(2), 251–268